Int. J. Solids Structures Vol. 17, No. 11, pp. 1085–1101, 1981
Printed in Great Britain.

0020-7683/81/111085-17$02.00/0

BIFURCATION ANALYSIS OF THE PLANE RECTILINEAR DEFORMATION ON DRY SAND SAMPLES

I. VARDOULAKIS
Department of Civil and Mineral Engineering, University of Minnesota, Minneapolis, MN 55455, U.S.A.

(*Received* 24 *September* 1980; *in revised form* 22 *January* 1981)

Abstract—Diffuse bifurcation modes of plane rectilinear deformations on dry sand samples are discussed. Sand is described by a Mohr–Coulomb, single hardening, rigid-plastic model, with a non-associated flow rule in which Rowe's stress-dilatancy principle is incorporated. The only significant diffuse bifurcation mode in the biaxial test with mixed boundary conditions is antisymmetric buckling before localization. In the strain controlled biaxial test internal buckling is possible everywhere in the hyperpolic regime.

INTRODUCTION

In this paper a bifurcation analysis of the biaxial test on dry sand samples is presented. This bifurcation problem is the soil mechanics counterpart of the metal plasticity problems analyzed by Hill and Hutchinson[1], Young[2] and more recently by Needleman[3]. The analysis is concentrated in the discussion of diffuse bifurcation modes since the shear band analysis is presented in previous publications by the author[4, 5]. For convenient reference the band analysis is outlined here because it simplifies the discussion of the diffuse modes[1].

The constitutive model used here is the so-called rigid-granular model, which is proposed for describing sand at low stress levels with respect to the elasticity and/or the strength of the soil grains. The rigid-granular concept appears first in Rowe's stress-dilatancy theory[6] and is theoretically extended by Dietrich[7] in the theory of 'psammic' material. A simplified form of the rigid-granular model, introduced by the author, has already yielded satisfactory results in the shear band analysis of the biaxial test[5] and in the shear band and diffuse modes analysis of the triaxial test on dry sand samples[8, 9]. The basic assumptions of this model are the following: (1) there is no material property with the dimension of stress, and (2) dilatancy is an internal constraint and consistently the mean pressure increment is statically indeterminate.

The rigid-granular model can be related to a double hardening model, like the one proposed by Lade[10] or more recently by Vermeer[11], if volumetric strain hardening is neglected. The present model is also very similar in structure to the one proposed by Stören and Rice[12] for metals and the one by Rudnicki and Rice[13] for fissured rocks. The structure of these models is duscussed by Needleman[13], who applies a non-dilatant, pressure sensitive model in the bifurcation analysis of plane strain tension and compression. Similar work has been also presented by the author in the bifurcation analysis of the biaxial and of the triaxial test[4, 5, 8, 9].

The bifurcation problem is formulated semi-inversely in terms of a perturbation solution. At the moment of bifurcation nearly proportional loading in the sense of Shanley[14] is assumed, i.e. this perturbation technique allows a linearization of the constitutive equations, which holds for small deviations from the "straight ahead" continuation of the preceding loading history (see Refs. 5, 8 and 13).

A Mohr-Coulomb hardening rule is assumed to be valid. The hardening rule is expressed in terms of dimensionless stress measures, and strain hardening is measured by the shearing intensity of the total strain. Several investigators, e.g.[10, 11], have proposed a deviation from the Mohr-Coulomb hardening rule by introducing a dependence on the mean pressure. The hardening rule contains then a factor of the form $(p/p_0)^a$, where p is the current mean pressure and p_0 is an arbitrary pressure (the exponent a is for $p_0 = 100\ \text{kN/m}^2$ between one third and one half). The arbitrarness of p_0 means that the above modifications are merely curve fittings and not constitutive equations. An influence of the stress level into the constitutive response is actually expected in either very high stress levels or for strain paths violating the dilatancy constraint.

The assumption that dilatancy is an internal constraint is a working hypothesis accompanied by the assumptions that the mean pressure increment is statically indeterminate. These material assumptions are to be checked in boundary value problems, where the class of solutions is not necessarily empty.

The present constitutive model is incomplete with respect to the instantaneous modulus μ for shearing parallel to the principal axes of prestress. This freedom allows us to solve the problem in terms of μ and consequently to cover a broad spectrum of constitutive assumptions[1]. For example, within a theory of plastic-flow like[10] or [11], μ equals the elastic shear modulus. For some deformation theories of plasticity, e.g. [9] and [12], μ equals the secant modulus of an adequate stress–strain curve. The secant modulus estimate for μ better fits the experimental results than the higher elastic value. For a granular soil μ cannot be an elastic constant; μ must depend on the governing stress level. Within the rigid-granular model μ is proportional to the governing mean stress and can be actually fitted as a modified secant modulus[5].

In the next chapter we discuss briefly the constitutive equations for dry sand and for plane strain conditions, utilizing the above mentioned rigid granular behavior. Subsequently the field equations, the band analysis and the classification of regimes are presented. Diffuse bifurcation modes of a biaxial test with mixed boundary conditions are then analyzed, and the corresponding eigenvalue equations for the physically significant cases are formulated. The eigenvalue equations are then numerically solved for special values of the material properties, which are characteristic for medium grained sand. Finally Biot's problem of internal buckling[15] is discussed as a possible diffuse bifurcation mode of a strain controlled biaxial test.

CONSTITUTIVE EQUATIONS

Let a homogeneous, cuboidal sand sample in an undistorted initial configuration C_0 be subjected to a smooth, quasi-static, homogeneous rectilinear deformation. We call the resultant configuration C. The boundaries of the sample in C are parallel to the principal axes of the Cauchy stress tensor σ_{ij} in C, Fig. 1(a, b). In the following analysis only the x_i-Cartesian coordinate system of the principal axes of σ_{ij} will be used.

For specifying further the constitutive response, the bifurcation problem is formulated semi-inversely in terms of a perturbation solution. The bifurcation mode is then a linear combination of a homogeneous rectilinear deformation and an inhomogeneous perturbation solution. Let C' be the configuration of the sample corresponding to the considered bifurcation mode, and let u_i be the corresponding infinitesimal displacement field. It is assumed that u_i has the following form:

$$u_i = u_i^0 + \eta \tilde{u}_i \quad (\eta \to 0). \tag{1}$$

u_i^0 is called the trivial mode and is assumed to be a rectilinear deformation (see Fig. 1c):

$$u_i^0 := q_{(i)} x_j \delta_{ij}. \tag{2}$$

$\tilde{u}_i$ is called the non-trivial mode and is a possible analytical description of the considered catastrophy form. The perturbation parameter η in (1) is a suitably small positive number ($\|u_i^0\|$ and $\|u_{i,j}^0\| \geqslant \eta > 0$. From (1) the infinitesimal strain tensor ϵ_{ij} and the infinitesimal rotation tensor ω_{ij} can be deduced:

$$\epsilon_{ij} = \frac{1}{2}(u_{i,j} + u_{j,i}); \quad \omega_{ij} = \frac{1}{2}(u_{i,j} - u_{j,i}), \tag{3}$$

where $(\cdot)_{,i}$ denotes differentiation with respect to the x_i-coordinate.

The plane strain condition is expressed here by the fact that the displacement vector and all its partial derivatives in the x_3-direction are vanishing:

$$u_3 = 0; \quad u_i = u_i(x_1, x_2) \quad (i = 1, 2). \tag{4}$$

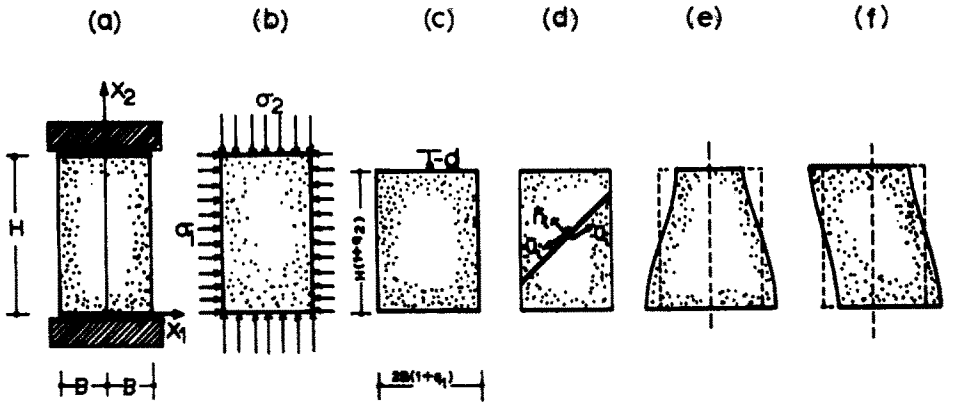

Fig. 1. (a) Biaxial test with mixed boundary conditions; (b) boundary stresses in C; (c) rectilinear deformation; (d) shear band bifurcation mode; (e) symmetric bifurcation mode (bulging); (f) antisymmetric bifurcation mode (buckling).

For a simple material $\sigma_{13} = \sigma_{23} = 0$. Let σ_3 be the principal stress normal to the plane of deformation, and let σ_1 and σ_2 be the other principal stresses in the plane of deformation, see Fig. 1(b). It is a well established experimental finding that for sand samples under plane strain conditions σ_3 is the intermediate principal stress. If σ_2 denotes the absolutely maximum principal stress, it is then

$$\sigma_2 < \sigma_3 < \sigma_1 < 0, \tag{5}$$

where *compression is taken as negative.*

In plane strain tests it is found that σ_3 is approximately proportional to the mean pressure in the plane[16]:

$$\sigma_3 \simeq \text{const.}\,(\sigma_1 + \sigma_2). \tag{6}$$

Let s and t denote the so-called Roscoe stress measures:

$$s := \frac{1}{2}(\sigma_1 + \sigma_2); \quad t := \frac{1}{2}(\sigma_1 - \sigma_2). \tag{7}$$

We assume that the perturbation solution $\eta\tilde{\epsilon}_{ij}$ is so small that the Mohr-Coulomb friction law is continuously valid. The Mohr–Coulomb yield condition can be expressed in terms of the mobilized friction angle ϕ_m defined by

$$\phi_m = \arcsin\left(-\frac{t}{s}\right). \tag{8}$$

$\sin\phi_m$ then obeys a strain-hardening rule:

$$\sin\phi_m = T(g), \tag{9}$$

where $T(\cdot)$ is a hardening function and g is a finite Eulerian measure of the shearing intensity of the deformation measured from the initial configuration C_0. g is defined as logarithmic strain:

$$g = \ln\left(\frac{B}{B_0}\right) - \ln\left(\frac{H}{H_0}\right), \tag{10}$$

where $2B$, $2B_0$ and H, H_0 are the width and the height of the sample in C and C_0 respectively; see Fig. 1(a).

The slope of the stress–strain curve (9) is called the dimensionless hardening rate h, given by

$$h = \frac{dT}{dg}. \tag{11}$$

The most important feature of the present constitutive model is expressed by means of a *non-associated* flow rule in which Rowe's stress-dilatancy principle is incorporated. The stress-dilatancy equation for the biaxial test reads [6]

$$\frac{\sigma_2 \epsilon_2}{\sigma_1 \epsilon_1} = -\lambda_c^2, \tag{12}$$

where λ_c^2 is the stress ratio in the state of isochoric deformation.

According to (6) the increment of isotropic pressure is proportional to the increment Δs of the mean pressure in the plane of deformation. Due to the assumed dilatancy constraint, the increment of isotropic pressure, and consequently Δs, are regarded as statically indeterminate quantities.

The constitutive equations are formulated in terms of the increment Δs_{ij} of the co-rotated Cauchy stress tensor. Δs_{ij} can be computed from the Cauchy stress increment $\Delta \sigma_{ij}$ according to the following equation [17]:

$$\Delta s_{ij} = \Delta \sigma_{ij} - \omega_{ik}\sigma_{kj} + \sigma_{ik}\omega_{kj}. \tag{13}$$

The constitutive equations for the considered infinitesimal transition $C \to C'$, derived by the author in [5], read:

$$\begin{aligned} \Delta s_{11} &= (1 - \sin \phi_m)\Delta s - sh(\epsilon_{11} - \epsilon_{22}) \\ \Delta s_{22} &= (1 + \sin \phi_m)\Delta s - sh(\epsilon_{22} - \epsilon_{11}) \\ \Delta s_{12} &= 2\mu \epsilon_{12} \\ \epsilon_{11} + \epsilon_{22} &= \sin \nu_m \sqrt{[(\epsilon_{11} - \epsilon_{22})^2 + 4\epsilon_{12}^2]}; \end{aligned} \tag{14}$$

where the last equation expresses the dilatancy constraint and ν_m is the mobilized dilatancy angle of the material. For the considered perturbation solution (1), (14) can be linearized as follows:

$$\epsilon_{11} = -\delta^2 \epsilon_{22} \tag{15}$$

where

$$\delta = \tan(45° + \nu_m/2). \tag{16}$$

Let λ^2 be the principal stress ratio in C, which is related to the mobilized friction angle ϕ_m according to well-known formula:

$$\lambda^2 = \frac{\sigma_2}{\sigma_1} = \tan^2(45° + \phi_m/2). \tag{17}$$

From (12), (15) and (17) there follows finally a simple formula for δ:

$$\delta = \frac{\lambda}{\lambda_c}. \tag{18}$$

FIELD EQUATIONS

The field equations for continued equilibrium for the considered infinitesimal transition $C \to C'$ are expressed in terms of the increment $\Delta \Sigma_{ij}$ of the 1. Piola–Kirchhoff stress tensor [17]:

$$\Delta\Sigma_{ij,j} = 0, \tag{19}$$

where the increment $\Delta\Sigma_{ij}$ can be expressed in terms of the constitutive stress increment Δs_{ij}, the prestress σ_{ij}, the infinitesimal strain ϵ_{ij} and the infinitesimal rotation tensor ω_{ij} according to the following formula[17]:

$$\Delta\Sigma_{ij} = \Delta s_{ij} + \omega_{ik}\sigma_{kj} - \sigma_{ik}\epsilon_{kj} + \sigma_{ij}\epsilon_{kk}. \tag{20}$$

For the considered state of prestress in C (see Ref. [15]), (19) reads:

$$\begin{aligned} \Delta s_{11,1} + \Delta s_{12,2} + 2t\omega_{21,2} &= 0 \\ \Delta s_{21,1} + \Delta s_{22,2} + 2t\omega_{21,1} &= 0. \end{aligned} \tag{21}$$

Substitution of the constitutive equations (14) into the above field equations yields the following field equations for the non-trivial mode $\tilde{u}_i$:

$$\begin{aligned} -(1-\sin\phi_m)\frac{\partial\Delta\tilde{s}}{\partial x_1} &= -sh\frac{\partial^2\tilde{u}_1}{\partial x_1^2} + \{(\mu+t)+sh\}\frac{\partial^2\tilde{u}_2}{\partial x_1\partial x_2} + (\mu-t)\frac{\partial^2\tilde{u}_1}{\partial x_2^2}, \\ -(1+\sin\phi_m)\frac{\partial\Delta\tilde{s}}{\partial x_2} &= -sh\frac{\partial^2\tilde{u}_2}{\partial x_2^2} + \{(\mu-t)+sh\}\frac{\partial^2\tilde{u}_1}{\partial x_1\partial x_2} + (\mu+t)\frac{\partial^2\tilde{u}_2}{\partial x_1^2}. \end{aligned} \tag{22}$$

Differentiation and combination of these field equation so as to eliminate $\Delta\tilde{s}$, which is statically indeterminate, yield one equation for the displacement components $\tilde{u}_1$ and $\tilde{u}_2$. Then a stream function $\Psi(x_1, x_2)$ may be introduced such that the dilatancy constraint (15) is automatically satisfied:

$$\tilde{u}_1 = \Psi_{,2}; \quad \tilde{u}_2 = -\frac{1}{\delta^2}\Psi_{,1}. \tag{23}$$

The resultant equation (see Ref. [15]) for Ψ reads:

$$\Psi_{,1111} + b\Psi_{,1122} + c\Psi_{,2222} = 0, \tag{24}$$

where

$$b = \left(a_0\frac{t}{\mu} + a_1\right)/(1 + t/\mu)$$

$$a_0 = -\lambda^2 + \delta^2 + ah, \quad a = 4/((1-\sin\phi_m)(1-\sin\nu_m)\sin\phi_m) \tag{25}$$

$$a_1 = -(\lambda^2 + \delta^2)$$

$$c = \lambda^2\delta^2\xi; \quad \xi = \frac{1 - t/\mu}{1 + t/\mu}. \tag{26}$$

Equation (24) is a 4th-order partial differential equation of the mixed type. In the present analysis only boundary value problems will be discussed for which the type of (24) is always the same everywhere in the considered body, (bifurcation analysis of the perfect specimen).

Remark

Recently Mehrabadi and Cowin[18] have discussed so-called "pre-failure" and "post-failure" solid plasticity models based mainly on the work of Rudnicki and Rice[13] and on the work of Spencer[19]. Since the stress state inside the shear band cannot be completely determined by direct measurements[20] only an elaborated post-localization analysis in the

sense, e.g. of Hutchinson and Tvergaard[21] could illuminate the "post-failure" behavior of the considered material. In such an analysis the elliptic/hyperbolic problem related to (24) is discussed by matching solutions along characteristics of the perfect solution[21]. Vardoulakis[20] has observed that shear bands in biaxial tests behave always contractant immediately after localization. This "inversion of dilatancy" and other directional phenomena observed, suggest the use in post-bifurcation analyses of constitutive models with kinematic hardening[22] or the use of incrementally non-linear models without yield surface[23]. As we mentioned above, post-bifurcation behavior will not be considered here.

Band analysis and classification of regimes

For convenient reference we outline here briefly the shear band bifurcation analysis Fig. 1(d), of the considered problem, which appeared in Refs. [4, 5]. The condition for the localization of the deformation into a shear band can be derived from the requirement that across a shear band boundary the internal and external stress vectors are in equilibrium. Generally the statical compatibility conditions read (see Ref. [13]):

$$[\Delta\Sigma_{ij}]\bar{n}_j = 0 \tag{27}$$

where $[\cdot]$ denotes the jump of a quantity across the shear boundary with the unit outward vector $\bar{n}_i$. The shear band boundaries are assumed to be stationary discontinuity surfaces of the displacement gradient. Across such a shear band boundary the following geometrical compatibility conditions hold[13]:

$$[u_{i,j}] = \bar{u}_i\bar{n}_j,$$

where $\bar{u}_i$ is proportional to the displacement vector at the shear band boundaries.

Substitution of (14), (20) and (28) into the statical compatibility conditions (27) yields:

$$\begin{aligned}(1-\sin\phi_m)[\Delta s] &= sh\bar{u}_1\bar{n}_1 - (sh+\sigma_1)\bar{u}_2\bar{n}_2 \\ &\quad -\frac{\bar{n}_2}{\bar{n}_1}\{(\mu-t)\bar{u}_1\bar{n}_2 + (\mu-s)\bar{u}_2\bar{n}_1\} \\ (1+\sin\phi_m)[\Delta s] &= -(sh+\sigma_2)\bar{u}_1\bar{n}_1 + sh\bar{u}_2\bar{n}_2 \\ &\quad -\frac{\bar{n}_1}{\bar{n}_2}\{(\mu-s)\bar{u}_1\bar{n}_2 + (\mu+t)\bar{u}_2\bar{n}_1\}.\end{aligned} \tag{29}$$

Eliminating $[\Delta s]$ from the above equations and using the dilatancy constraint (15) yield the following well-known form of the localization condition:

$$\bar{n}_1^4 + b\bar{n}_1^2\bar{n}_2^2 + c\bar{n}_2^4 = 0, \tag{30}$$

where b and c are given by (25) and (26).

The three possibilities of the solution of (30) can be classified as follows[1]:

E(elliptic): no real $\bar{n}_1/\bar{n}_2$

P(parabolic): 2 real $\bar{n}_1/\bar{n}_2$

H(hyperbolic): 4 real $\bar{n}_1/\bar{n}_2$.

The localization condition (30) can be written in the form

$$\left(\frac{\bar{n}_1}{\bar{n}_2}\right)^2 = \frac{1}{2}(-b \pm \sqrt{D}), \tag{31}$$

where

$$D = \{A_0(t/\mu)^2 + A_1(t/\mu) + A_2\}/(t/\mu + 1)^2 \tag{32}$$

and

$$A_0 = (ah - \lambda^2 + \delta^2)^2 + 4\lambda^2\delta^2 > 0,$$

$$A_1 = -2(\lambda^2 + \delta^2)(ah - \lambda^2 + \delta^2),$$

$$A_2 = (\lambda^2 - \delta^2)^2. \tag{33}$$

The discriminant D, given by (32), can be looked upon as a rational function of t/μ. The sign of D depends on the sign of the discriminant

$$\Delta = A_1^2 - 4A_0A_2 = 16a^2\lambda^2\delta^2h(h - h_R), \tag{34}$$

where

$$h_R = \sin\phi_m(\sin\phi_m - \sin\nu_m). \tag{35}$$

h_R (R for Roscoe[5]) is always positive. This is a direct consequence of normality not holding for granular material, expressed by the inequality

$$\phi_m > \nu_m. \tag{36}$$

Note that the hardening rate at the peak of the stress-strain curve $T(g)$ is denoted by h_C (C for Coulomb[5]):

$$h_C = 0. \tag{37}$$

For $h \geqslant h_R$, $D(t/\mu) = 0$ has always two positive roots, ρ_1 and ρ_2:

$$\rho_{1/2} = \frac{(\lambda^2 + \delta^2)a(h - h_R/2) \mp 2\lambda\delta a\sqrt{[h(h - h_R)]}}{a^2(h - h_R/2)^2 + 4\lambda^2\delta^2}. \tag{38}$$

Due to $A_0 > 0$ one has

$$D < 0 \text{ for } \rho_1 < t/\mu < \rho_2. \tag{39}$$

On the other hand the coefficient b in (30) can be written in the form

$$b = a(h - h_R/2)\frac{t/\mu - q}{t/\mu + 1}, \tag{40}$$

where

$$q = \frac{h_M}{2h - h_R}; \quad h_M = \sin\phi_m(1 - \sin\phi_m\sin\nu_m). \tag{41}$$

The corresponding characteristic regimes of (30) are sketched in Fig. 2, in a (t/μ) vs h plot.

According to the proposition of Hill and Hutchinson[1], it is assumed that localizations occur on the $E|H$-boundary between E and H.

In order to suppress localization outside E several investigators have developed purely strain controlled tests[24, 25], see Fig. 7. However, Rice [26] has shown that it is always

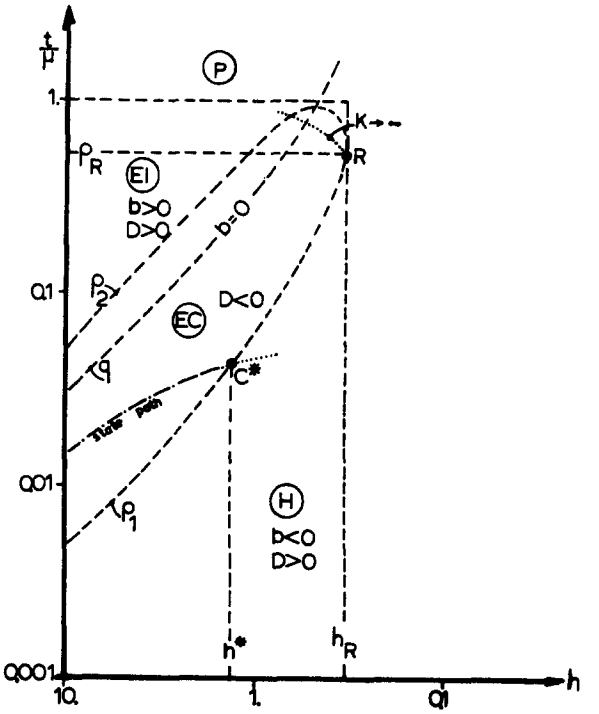

Fig. 2. Characteristic regimes of the localization condition.

possible to construct shear band solutions compatible with all around displacement boundary conditions. This possibility is verified experimentally for fine grained materials like fine sand, silt or clay[24].

Note that the parabolic regime can be identified for the case $t/\mu > 1$,[1, 27]. If μ is a secant-type modulus, the above inequality is true for large shear strains in the order of magnitude of 100%. For such big shear strains, sand always reaches the critical state. This means that the consideration of the parabolic regime is only significant if plastic flow in the critical state is considered. The *E*/*P*-boundary and the *P*-regime will not be considered here.

In the following analysis two types of diffuse bifurcation problems will be discussed: (1) buckling and bulging and bulging modes, which are significant in a biaxial test with mixed boundary conditions, and (2) internal buckling modes which are significant in a strain controlled biaxial test.

DIFFUSE MODES FOR MIXED BOUNDARY CONDITIONS

In this chapter we consider the physically significant bifurcation modes in the biaxial test with mixed boundary conditions and non-tilting top platen; see Fig. 1(a, e and f). Note that for tilting top platen the dominant diffuse bifurcation mode is a bending one[4, 20]. On the edge $x_2 = H$ of the sample, a uniform displacement d is prescribed while the displacement on the cdge $x_2 = 0$ and the shear stresses on both edges are vanishing. The sides $x_2 = \pm B$ are subjected to a hydrostatic confining pressure $\sigma_1 = -\sigma_c$. As already mentioned the trivial mode u°_i is a rectilinear deformation, expressed by (2). It is assumed that u°_i satisfies the kinematic boundary conditions (Fig. 1c):

$$u^\circ_2(x_1, 0) = 0; \quad u^\circ_2(x_1, H) = d. \tag{42}$$

For the non-trivial mode the following displacement field is tested:

$$\tilde{u}_1 = \hat{u}(\chi)\cos\psi; \quad \tilde{u}_2 = \hat{v}(\chi)\sin\psi \tag{43}$$

with

$$\chi = \frac{x_1}{B}, \quad \psi = m\pi\frac{x_2}{H} \ (m = 1, 2, \ldots). \tag{44}$$

This field automatically satisfies the homogeneous boundary conditions at the ends of the sample:

$$\tilde{u}_2(x_1, 0) = \tilde{u}_2(x_1, H) = 0; \ \tilde{\epsilon}_{12}(x_1, 0) = \tilde{\epsilon}_{12}(x_1, H) = 0. \tag{45}$$

From (23) and (43) it follows that the appropriate stream function reads

$$\Psi = \frac{B}{K}\hat{u}(\chi)\sin\psi, \tag{46}$$

where

$$K = m\pi\frac{B}{H} \tag{47}$$

characterizes the physical slenderness of the sample.

Using (23) and (46), the following expressions can be derived:

$$\begin{aligned} \tilde{\epsilon}_{11} - \tilde{\epsilon}_{22} &= \frac{1}{B\delta^2}(1+\delta^2)\hat{u}'\cos\psi \\ 2\tilde{\epsilon}_{12} &= \frac{-1}{BK\delta^2}(\hat{u}'' + K^2\delta^2\hat{u})\sin\psi, \\ 2\tilde{\omega}_{21} &= \frac{-1}{BK\delta^2}(\hat{u}'' - K^2\delta^2\hat{u})\sin\psi \end{aligned} \tag{48}$$

where $(\cdot)'$ denotes differentiation with respect to the dimensionless height-coordinate χ.

The following representation of the mean pressure increment $\Delta\tilde{s}$ is consistent with the displacement field (43) introduced above:

$$\Delta\tilde{s} = \hat{s}(\chi)\cos\psi. \tag{49}$$

From $(22)_2$ it follows that

$$\hat{s} = \frac{-1}{1+\sin\phi_m}\cdot\frac{1}{BK^2\delta^2}\{(\mu+t)\hat{u}''' + K^2[\delta^2(\mu-t) + (1+\delta^2)sh]\hat{u}'\}. \tag{50}$$

Substitution of Ψ from (46) into (24) yields finally the well-known governing differential equation for the considered bifurcation problem [1–3]:

$$\hat{u}^{IV} - K^2 b\hat{u}'' + K^4 c\hat{u} = 0. \tag{51}$$

The solution of (51) is of the form

$$\hat{u}(\chi) = \sum_{j=1}^{4} C_j \exp\{K\alpha_j\chi\}, \tag{52}$$

where α_j satisfies the characteristic equation

$$\alpha_j^4 - b\alpha_j^2 + c = 0. \tag{53}$$

When α is replaced by $i\alpha$, where $i = \sqrt{(-1)}$, the above characteristic equation transforms into an equation similar to (30). The character of the roots of (53) depends on whether the state variables lie in the elliptic or in the hyperbolic regime of (30).

Boundary conditions

For the considered infinitesimal transition $C \to C'$, the confining pressure σ_c is assumed to remain constant. The boundary conditions for the unconfined sides of the sample ($\chi = \pm 1$) express the fact that a traction of constant intensity always acts normally on these boundaries. Mathematically this condition reads

$$\Delta\Sigma_{ij} n_j = \sigma_c (n_k \delta_{il} - n_i \delta_{kl}) u_{k,l} \tag{54}$$

where $\{n_i\}^T = \{\pm 1, 0, 0\}$ is the outwards boundary normal. Substitution from (20) and (14) into (54) yields for

$$\chi = \pm 1 \quad 2(\mu + t)\bar{\epsilon}_{12} = 0; \quad \Delta\bar{s}_{11} = 0. \tag{55}$$

Using (14) and (48)–(50) the boundary conditions may be expressed in terms of $\hat{u}$; i.e. for $\chi = \pm 1$,

$$\begin{aligned} \bar{\epsilon}_{12} &= 0; \quad \hat{u}'' + K^2\delta^2\hat{u} = 0 \\ \Delta\bar{s}_{11} &= 0: \quad \hat{u}''' + K^2 P\hat{u}' = 0, \end{aligned} \tag{56}$$

where

$$P = \left\{ -(\delta^2 + ah)\frac{t}{\mu} + \delta^2 \right\} / (1 + t/\mu). \tag{57}$$

Symmetric bifurcation modes are characterized by the condition: $\hat{u}(\chi) = -\hat{u}(-\chi)$, Fig. 1(e). In this case is the solution (52), $C_3 = C_4 = 0$; i.e.

$$\hat{u}_{sym} = C_1\hat{u}_{(1)} + C_2\hat{u}_{(2)}. \tag{58}$$

The bifurcation condition can be derived from the homogeneous boundary conditions (56), if we ask for non-trivial solutions for C_1 and C_2. For $\chi = 1$ (56) and (58) yield

$$\{\hat{u}'''_{(1)} + K^2 P\hat{u}'_{(1)}\}\{\hat{u}''_{(2)} + K^2\delta^2\hat{u}_{(2)}\} = \{\hat{u}'''_{(2)} + K^2 P\hat{u}'_{(2)}\}\{\hat{u}''_{(1)} + K^2\delta^2\hat{u}_{(1)}\}. \tag{59}$$

Antisymmetric bifurcation modes are characterized by the condition: $\hat{u}(\chi) = \hat{u}(-\chi)$, Fig. 1(f). The bifurcation condition for $\chi = 1$ is expressed by (59) by replacing the subscripts (1) and (2) by (3) and (4), respectively.

EIGENVALUE EQUATIONS IN THE E-REGIME

The assumption that the incipient shear modulus μ is a secant-type modulus means that μ decreases monotonously during the deformation $C_0 \to C$ and that it remains always positive. On the other hand the stress difference t is also positive and increases primarily until reaching a maximum value beyond the peak of the considered stress–strain curve $T(g)$. [It can be shown that the maximum load condition in the biaxial test with constant confining pressure and for a hypothetical homogeneous rectilinear deformation is attained in the softening regime for $h = -(1/2)(1 + \sin\nu_m)(1 - \sin\phi_m)\sin\phi_m$.] This means that t/μ must be a positive, monotonously increasing and convex function of h in the hardening regime. The actual state path $C_0 \to C$ in the state space $(t/\mu, h)$ must for consistency lie in the elliptic regime before failure, see Fig. 2. At some critical state C^* that state path will intersect the $E|H$-boundary. At the moment of intersection localization is possible and it is also assumed that it actually occurs. Note that the

theoretical predictions for the shear band inclination, based on the above model, were in good agreement with the experimental data[5]. The search of diffuse modes of the form (43) is therfore physically meaningful in E and on the E/H-boundary. In H, diffuse modes are only significant in strain-controlled tests, where it is always possible that diffuse and localized modes develop simultaneously. Such diffuse modes in H will be discussed separately in a later chapter.

The elliptic regime E, shown in Fig. 2, is divided into two subregimes: the elliptic complex subregime EC and the elliptic imaginary subregime EI[3]. In EC the roots of (30) are complex conjugate pairs, while in EI they are purely imaginary.

The EC-subregime

This subregime is given by the inequalities

$$h > h_R;\ \rho_1 < \frac{t}{\mu} < \rho_2. \tag{60}$$

The solutions of (51) are $e^{\pm z}$ and $e^{\pm t}$, where

$$z = K\alpha\chi;\quad \alpha = M + iN;\quad i = \sqrt{(-1)},$$

$$M = \sqrt{\left(\frac{1}{2}\left(\sqrt{(c)} + \frac{b}{2}\right)\right)};\quad N = \sqrt{\left(\frac{1}{2}\left(\sqrt{(c)} - \frac{b}{2}\right)\right)}. \tag{61}$$

The symmetric solutions are given by

$$\hat{u}_{(1)} = Re\{\sin \mathrm{h}\, z\} = \sin \mathrm{h}\,(KM\chi)\cos(KN\chi)$$

$$\hat{u}_{(2)} = Im\{\sin \mathrm{h}\, z\} = \cos \mathrm{h}\,(KM\chi)\sin(KN\chi), \tag{62}$$

and the antisymmetric solutions are given by

$$\hat{u}_{(3)} = Re\{\cos \mathrm{h}\, z\} = \cos \mathrm{h}\,(KM\chi)\cos(KN\chi)\ .$$

$$\hat{u}_{(4)} = Im\{\cos \mathrm{h}\, z\} = \sin \mathrm{h}\,(KM\chi)\sin(KN\chi). \tag{63}$$

Introducing (62) or (63) into the bifurcation condition (59), one asserts the following eigenvalue equation, see Refs. [1–3]:

$$\frac{\sin \mathrm{h}(2KM)}{\sin\,(2KN)} = \pm\frac{M}{N}\frac{\lambda\delta + \sqrt{\xi}(\delta^2 + ah/2)}{\lambda\delta - \sqrt{\xi}(\delta^2 + ah/2)}, \tag{64}$$

where, as throughout this chapter when two signs appear, the $(+)$ sign applies for the symmetric modes and the $(-)$ sign applies for the antisymmetric modes.

The EI-subregime

This subregime is given by the inequalities

$$h > h_R;\quad t/\mu > \max\{\rho_2, q\}. \tag{65}$$

In this case the solutions of (51) read:

$$\hat{u}_{(1)} = \sin \mathrm{h}(K\alpha\chi);\quad \hat{u}_{(2)} = \sin \mathrm{h}(K\beta\chi)$$

$$\hat{u}_{(3)} = \cos \mathrm{h}(K\alpha\chi);\quad \hat{u}_{(4)} = \cos\, \mathrm{h}(K\beta\chi),$$

where

$$\alpha = \sqrt{\left(\frac{1}{2}(b + \sqrt{D})\right)}; \quad \beta = \sqrt{\left(\frac{1}{2}(b - \sqrt{D})\right)}. \tag{67}$$

The eigenvalue equation reads:

$$\left\{\frac{\tan h(K\beta)}{\tan h(K\alpha)}\right\}^{\pm 1} = \frac{\beta}{\alpha}\frac{(\alpha^2 + \delta^2)(\beta^2 + P)}{(\alpha^2 + P)(\beta^2 + \delta^2)}. \tag{68}$$

The E/H- and the EC/EI-boundary

The boundaries are characterized by the condition $D = 0$. On the E/H-boundary the eigenvalue equation takes the form,

$$\frac{\sin(2K^4\sqrt{(c_1)})}{2K^4\sqrt{(c_1)}} = \pm\frac{(\sqrt{(c_1)} - \delta^2)(\sqrt{(c_1)} - P_1)}{(3\sqrt{(c_1)} - P_1)(\sqrt{(c_1)} - \delta^2) - 2\sqrt{(c_1)}(\sqrt{(c_1)} - P_1)}, \tag{69}$$

where c_1 and P_1 are the values of c and P, respectively, for $t/\mu = \rho_1$; see (26) and (57). On the EC/EI-boundary the eigenvalue equation reads:

$$\frac{\sin h(2K^4\sqrt{(c_2)})}{2K^4\sqrt{(c_2)}} = \pm\frac{(\sqrt{(c_2)} + \delta^2)(\sqrt{(c_2)} + P_2)}{(3\sqrt{(c_2)} + P_2)(\sqrt{(c_2)} + \delta^2) - 2\sqrt{(c_2)}(\sqrt{(c_2)} + P_2)}, \tag{70}$$

where c_2 and P_2 are the values of c and P, resepctively, for $t/\mu = \rho_2$. For $t/\mu = \rho_1$, (69) yields the lowest critical slenderness corresponding to some given hardening rate h:

$$K_{cr} = \min_{E}(K). \tag{71}$$

For $h = h_R$ the two bifurcation roots expressed by (38) coincide, and their common value, denoted by ρ_R, reads:

$$\rho_R = \frac{\lambda^2 - \delta^2}{\lambda^2 + \delta^2}. \tag{72}$$

For $\rho_1 = \rho_R$, $\sqrt{c} = \delta^2$ and (69) yield the maximum of the lowest critical slenderness:

$$\max K_{cr} = \frac{\pi}{2\delta^2}. \tag{73}$$

Equation (73) reflects the fact that dense, dilatant samples are less sensitive to diffuse bifurcation than loose, less dilatant or contractant samples. As it will be demonstrated in the next chapter, (73) represents a fairly conservative lower bound for the critical slenderness; see Fig. 5.

Short wave length limit

The bifurcation mode corresponding to the short wave length limit [3] can be computed from (64) and (68) by setting $K \to \infty$ ($m \to \infty$; see (47)) which yields the following eigenvalue equation

$$\sqrt{\xi} = \frac{\lambda\delta}{\delta^2 + ah/2}. \tag{74}$$

For $h = h_R$ (74) yields $t/\mu = \rho_R$ and for $h \to \infty$ the short wave length limit approaches the E/P-boundary from the interior of E; see Fig. 2. For overcritically dense sand specimens the shear band obliquities measured are always higher than the corresponding ones for $t/\mu > \rho_R$ [5]. Accordingly for overcritically dense sand specimens the shear band bifurcation is not initiated by small imperfections in the geometry of the specimen but probably by imperfections in the porosity distribution which cause local variations of the soil stiffness. In contrary for undercritically dense specimens ($t/\mu \to 1$) a sensitivity in surface imperfections is to be expected.

COMPUTATIONAL RESULTS

The eigenvalue equations (64), (68), (69) and (70) are evaluated for some sets of material properties which are characteristic for over-critically dense, medium grained sand. This special choice of material properties is made in order to compare the computational results with the experimental fildings [4, 5, 27]. The computations showed that the analysis can be restricted in the vicinity of the peak of the assumed stress–strain curves. This is because the computational critical slenderness at states with high hardening rates are extremely low. In the vicinity of the peak the mobilized friction angle ϕ_m and the mobilized dilatancy angle ν_m are approximately equal to their peak values ϕ_p and ν_p, respectively. According to Rowe [6] the stress ratio λ_c^2 in (12) is set equal to the one in the critical state:

$$\lambda_c = \tan(45° + \phi_c/2), \tag{75}$$

$$\varphi_c = 34° \tag{76}$$

is the critical friction angle of the considered sand [4, 5, 27]. Table 1 summarizes the material properties for two characteristic porosities of the considered sand [5].

The range of variation of the hardening rate h is linked to the experimental finding in the biaxial tests with the considered sand that localization appeared for critical hardening rates h^*, estimated by the following equation [27]:

$$h^* \simeq 2.5/(1 + \delta^2). \tag{77}$$

Figures 3 and 4 show the computational results for antisymmetric bifurcation in E for dense and medium dense sand samples. The corresponding eigenvalue equations are solved iterratively in terms of the engineering slenderness $2B/H$ by scanning the elliptic regime in the range $h_R < h < 2$, $\rho_1 \le t/\mu < 1$. The results are plotted in (t/μ vs h)-diagrams, where contours of constant slenderness are depicted. By comparing Fig. 3 and Fig. 4, it follows that medium dense samples are more sensitive to diffuse buckling than dense ones. For h^* estimated from (77), only very slender samples will show diffuse buckling. This result is supported from the experimental evidence that for dense and medium dense samples no buckling was observed [4, 5, 27]. For the medium dense samples with $2B/H = 0.32$ at peak and $h^* = 1.14$ from (77), the minimum critical slenderness according to (69) is 0.33. This means that diffuse buckling can only develop in the vicinity of the E/H-boundary. By passing the E/H-boundary, shear bands are formed. Consequently the development of the diffuse mode is interrupted at its beginning.

The lowest critical slenderness, $(2B/H)_{cr}$, for antisymmetric bifurcation is computed in the range $h_R \le h < 2$ and for the two sets of material properties listed in Table 1. The results are

Table 1. Material properties for some characteristic initial porosities n_0 of a medium grained sand; see Ref. [5] and eqns (18), (75) and (76)

Classification (n_0)	ϕ_p (°)	ν_p (°)
dense sand (36%)	47.	16.9
medium dense sand (43%)	38.	4.9

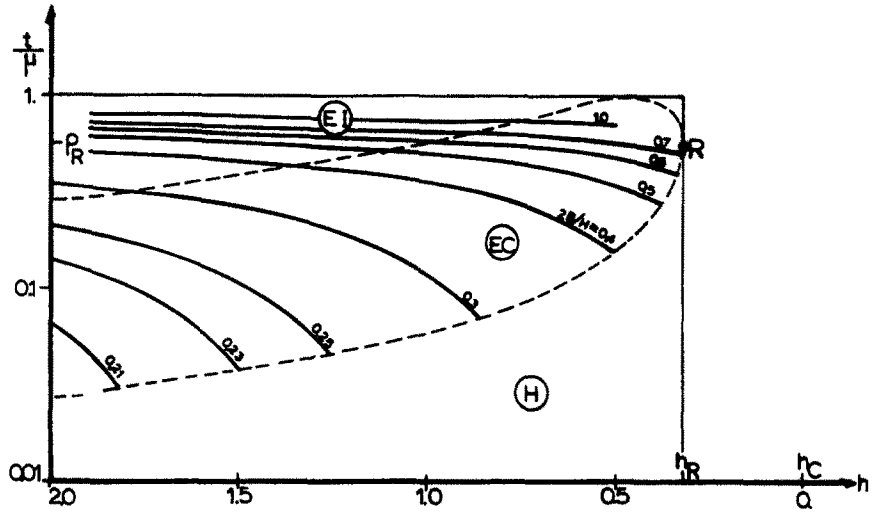

Fig. 3. Diffuse antisymmetric bifurcation modes in the elliptic regime; dense sand.

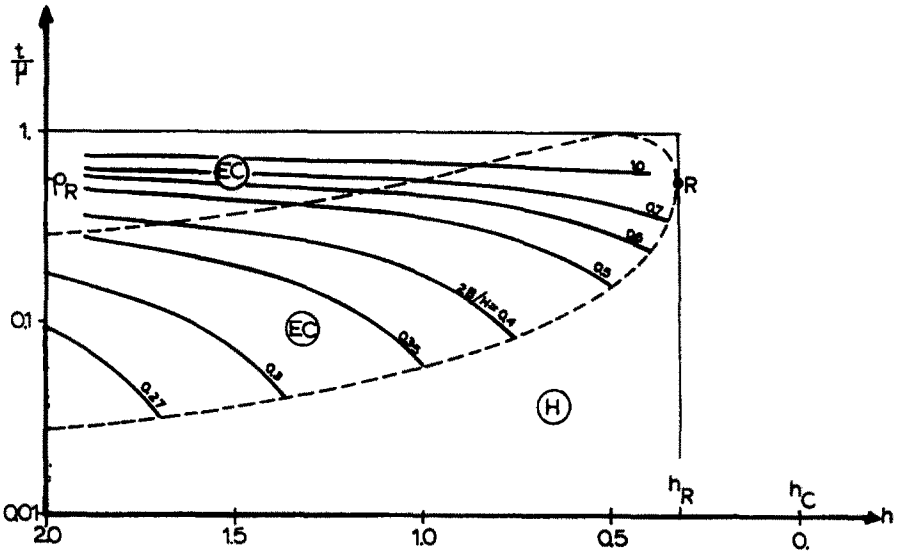

Fig. 4. Diffuse antisymmetric bifurcation modes in the elliptic regime; medium dense sand.

shown in Fig. 5 in a $(2B/H)_{cr}$ vs h plot. According to this figure, $(2B/H)_{cr}$ increases with increasing porosity and depends sensitively on the hardening rate h. This sentivity is much more pronounced as h approaches its limiting value h_R. As shown in Fig. 2, the critical hardening rate h^* is determined by the intersection of the actual state path and the E/H-boundary. Consequently the results shown in Fig. 5 actually reflect the sensitivity of the bifurcation solution on the actual value of the incipient shear modulus μ.

A typical result concerning the symmetric bifurcation modes is shown in Fig. 6. It follows from this figure that bulging is not significant in the biaxial test.

INTERNAL BUCKLING IN A STRAIN CONTROLLED TEST

In a strain controlled test like the one sketched in Fig. 7, the bifurcation modes shown in Fig. 1(d)–(f) are kinematically impossible. For that reason this test has been proposed for performing homogeneous deformations throughout [24, 25]. As we mentioned above shear bands cannot be suppressed in general by pure kinematic control [26]. In the following we shall consider the possibility of also diffuse modes in the strain controlled test. In a test like this, for reaching the limiting condition and passing into the softening regime of the hardening rule, the

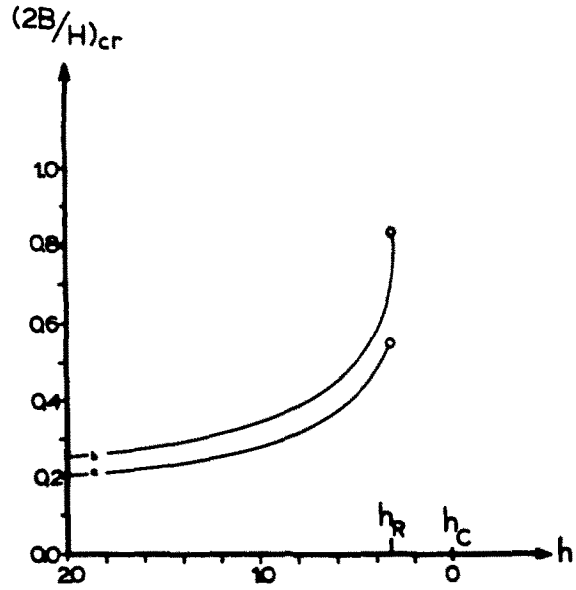

Fig. 5. Lowest critical slenderness for diffuse antisymmetric bifurcation modes: (a) dense sand; (b) medium dense sand.

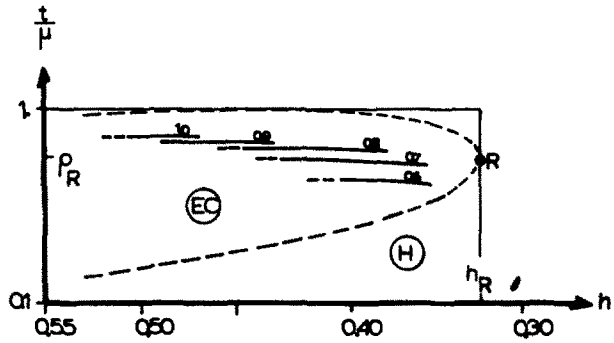

Fig. 6. Diffuse symmetric bifurcation modes in the EC-subregime; dense sand.

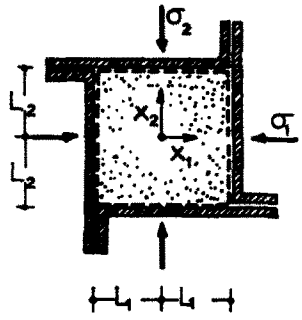

Fig. 7. The strain controlled biaxial test.

strain rates must always satisfy the momentaneous dilatancy constraint; see Goldscheider[28]. Under these circumstances Biot's problem of internal buckling[1, 15] is meaningful and can be formulated within the framework of the above illustrated perturbation analysis. For

$$\Psi = C\cos(\chi_n)\cos(\psi_m), \qquad C = u_0 / \left(\frac{m\pi}{2L_2}\right), \tag{78}$$

where

$$\chi_n = \frac{n\pi}{2}\frac{x_1}{L_1} \quad \psi_m = \frac{m\pi}{2}\frac{x_2}{L_2} \tag{79}$$

the non-trivial displacement field reads:

$$\tilde{u}_1 = -u_0 \cos(\chi_n)\sin(\psi_m); \quad \tilde{u}_2 = \frac{u_0}{\delta^2} r \sin(\chi_n)\cos(\psi_m), \tag{80}$$

with

$$r = \frac{n}{m}\frac{L_2}{L_1}. \tag{81}$$

For odd numbers n and m this displacement field satisfies the following homogeneous boundary conditions.

for

$$x_1 = \pm L_1: \quad \tilde{u}_1 = 0, \quad \tilde{\epsilon}_{12} = 0$$

for

$$x_2 = \pm L_2: \quad \tilde{u}_2 = 0, \quad \tilde{\epsilon}_{12} = 0. \tag{82}$$

introducing Ψ from (78) into (24) yields

$$r^4 + br^2 + c = 0, \tag{83}$$

The characteristic equation (83) is similar to the characteristic equation (30) for the shear band analysis. Consequently (83) possesses one pair of symmetric solution for r on the $E|H$ boundary and two pairs of symmetric solutions in H. It should be noted that the characteristic directions (31) are zero extension directions for the displacement field (80). Consequently it is possible that internal shear bands and internal buckling develop simultaneously.

CONCLUDING REMARKS

The present analysis has yielded the theoretical background to the working hypothesis that the biaxial test with mixed boundary conditions and non-tilting top platen performs homogeneous deformations until failure. The analysis shows that this hypothesis is true for overcritically dense specimens if these specimens are not extremely slender. Since the state of failure is that of the localization of the deformation into a shear band, a homogeneous rectilinear deformation can be performed in a biaxial test with mixed boundary conditions up to states very close to the peak.

On the other hand the strain-controlled biaxial test could allow for homogeneous, rectilinear deformations also in the hyperbolic regime if the specimen were perfectly homogeneous and if internal shear bands and Biot's internal buckling do not develop. The analysis indicates, however that both bifurcation modes are to be expected. Whether internal shear bands and/or internal buckling actually develop or not, cannot be answered definitely on the basis of the present bifurcation analysis. The behavior in the hyperbolic regime of a sand specimen in a strain-controlled test will be easier to analyse if precise measurements of the strain field are known.

REFERENCES

1. R. Hill and J. W. Hutchinson, Bifurcation phenomena in the plane tension test. *J. Mech. Phys. Solids* **23**, 239–264 (1975).
2. N. J. B. Young, Bifurcation phenomena in the plane compression test. *J. Mech. Phys. Solids* **24**, 77–91 (1976).
3. A. Needleman, Non-normality and bifurcation in plane strain tension and compression. *J. Mech. Phys. Solids* **27**, 231–254 (1979).

4. I. Vardoulakis, M. Goldscheider and G. Gudehus, Formation of shear bands in sand bodies as a bifurcation problem. *Int. J. Numer. Anal. Meth. Geomech.* 2, 99–128 (1978).
5. I. Vardoulakis, Shear band inclination and shear modulus of sand in biaxial tests. *Int. J. Numer. Anal. Meth. Geomech.* 4, 103–119 (1980).
6. P. W. Rowe, Theoretical meaning and observed values of deformation parameters for soil. *Proc. Roscoe Mem. Symp.*, (Edited by R. H. G. Perry) Cambridge University pp. 143–194 (1971).
7. Th. Dietrich, A comprehensive mechanical model of sand at low stress level, constitutive equations of soils, Preprints of Specialty Section 9, *IXth ICSMFE.* Tokyo, pp. 33–44 (1976).
8. I. Vardoulakis, Bifurcation analysis of the triaxial test on sand samples. *Acta Mechanica* 32, 35–54 (1979).
9. I. Vardoulakis, Constitutive properties of dry sand, observable in the triaxial test. *Acta Mechanica* 38, 219–239 (1981).
10. P. V. Lade, Elasto-plastic stress–strain theory for cohesionless soil with curved yield surfaces. *Int. J. Solids Structures* 13, 1019–1035 (1977).
11. P. A. Vermeer, A double hardening model for sand. *Géotechnique* 28, 413–433, (1978).
12. S. Stören and J. R. Rice, Localized necking in thin sheets. *J. Mech. Phys. Solids* 23, 421–441 (1975).
13. J. W. Rudnicki and J. R. Rice, Conditions for the localization of the deformation in pressure-sensitive dilatant materials. *J. Mech. Phys. Solids* 23, 371–394 (1975).
14. F. R. Shanley, Inelastic column theory. *J. Aeronaut. Sci.* 14, 261–268 (1974).
15. M. A. Biot, *Mechanics of Incremental Deformations.* Wiley, New York (1965).
16. D. H. Cornforth, Some experiments on the influence of strain conditions on the strength of sand. *Géotechnique* 14, 143–167 (1967).
17. C. Truesdell and W. Noll, Non-linear field theories of mechanics. *Flügge's Handbuch der Physik*, III/3, Springer (1965).
18. M. M. Mehrabadi and S. C. Cowin, Prefailure and post-failure soil plasticity models. *ASCE J. Engng Mech. Div. Proc.* 106, 991–1003 (1980).
19. A. J. M. Spencer, A theory of the kinematics of ideal soils under plane strain conditions. *J. Mech. Phys. Solids* 12, 337–351 (1964).
20. I. Vardoulakis and M. Goldscheider, A Biaxial apparatus for testing shear bands in soils. *Xth ICSMFE* 1981, Stockholm, to appear.
21. J. W. Hutchinson and V. Tvergaard, Shear band formation in plane strain. *Rep.*, Harvard University (1980).
22. Z. Mróz, On hypoelasticity and plasticity approaches to constitutive modelling of inelastic behaviour of soils. *Int. J. Numer. Anal. Meth. Geomech.* 4, 45–55 (1980).
23. D. Kolymbas and G. Gudehus, A constitutive law for sands and clays–position, prediction, evaluation. NSF/NSERC North American Workshop on *Plasticity Theories and Generalized Stress–Strain modeling of Soils*, McGill University, Montreal, Canada (1980).
24. E. C. Hambly, Plane strain behavior of remoduled normally consolidated kaolin. *Géotechnique*, 22, 301–317 (1972).
25. M. Goldscheider and G. Gudehus, Rectilinear extension on dry sand: Testing apparatus and experimental results. *Proc. VIIth ICSMFE* 1973, Moscow, 1/21, pp. 143–149 (1973).
26. J. R. Rice, The localization of plastic deformation. *Proc.*, 14*th IUTAM Cong.*, Delft, pp. 207–220 (1976).
27. I. Vardoulakis, Sherfugenbildung in Sandkörpern als Verzweigungsproblem, Veröffenthichungen des Instituts für Boden-und Felsmechanik, Universität Karlsruhe, Heft 70 (1977).
28. M. Goldscheider, Dilatanzverhalten von Sand bei geknickten Verformungswegen. *Mech. Res. Commun.* 2, 143–148 (1975).